Radiation, Joule Heating, Viscous Dissipation, and Soret-Dufour Effects on MHD Oscillatory Flow in a Channel Filled with Porous Medium in the Presence of Chemical Reaction

Dr. G. Prabhakara Rao

Lecturer in Mathematics, Government College (A), Anantapur, Andhra Pradesh, India-515001
Email: *nari.prabhu[at]gmail.com*

Abstract: ***This study examines unsteady oscillatory magnetohydrodynamic free-convection flow of an electrically conducting viscous fluid in a porous channel with coupled heat and mass transfer. The mathematical model incorporates thermal radiation, heat source/sink, Joule heating, viscous dissipation, the Soret and Dufour effects, and a first-order chemical reaction. The governing dimensionless momentum, energy, and concentration equations are solved numerically in Mathematica using NDSolve Value with the Method of Lines under an oscillatory pressure-gradient forcing. No-slip conditions are imposed on both channel walls, while the wall temperature and concentration are held constant. The computed solutions provide transient velocity, temperature, and concentration distributions, along with histories of wall skin friction, Nusselt number, and Sherwood number. The parametric study shows that magnetic damping suppresses the axial velocity, whereas buoyancy and permeability enhance the flow. Radiation, heat generation, viscous dissipation, Joule heating, and Dufour coupling elevate the temperature field and thicken the thermal layer. The Soret parameter enhances species diffusion driven by temperature gradients, while chemical reactions reduce concentration and attenuate solutal buoyancy. The combined action of porous resistance, magnetic braking, and cross-diffusion substantially alters transport rates at the channel walls. The model is relevant to oscillatory transport in porous thermal systems, electromagnetic processing, biomedical flows, and chemically reactive heat-transfer devices.***

Keywords: Magnetohydrodynamic oscillatory flow; porous channel; thermal radiation; Joule heating; viscous dissipation; Soret effect; Dufour effect; chemical reaction; heat and mass transfer; Method of Lines

1. Introduction

Magnetohydrodynamic (MHD) flow in porous media-filled channels has attracted considerable attention for its wide range of applications in engineering, geophysics, energy systems, and biomedical transport processes. The interaction between an electrically conducting fluid and an applied magnetic field provides an effective means of controlling momentum, heat, and mass transfer in such systems. Oscillatory channel flow is particularly important because periodic forcing is common in pulsatile pumping devices, thermal systems, biomedical flows, and industrial transport operations. As a result, the study of MHD oscillatory flow through porous channels remains an important area of research in fluid dynamics and heat transfer. Earlier works by Makinde and Mhone [29], Muthuraj and Srinivas [30], and Misra and Adhikary [28] have shown that magnetic fields and porous medium resistance significantly affect velocity and thermal characteristics in oscillatory channel flows.

In many practical situations, heat and mass transfer in MHD flows are influenced by additional physical mechanisms that cannot be neglected. Among these, thermal radiation plays a major role in high-temperature environments, including combustion systems, nuclear engineering, thermal insulation, gas turbines, and astrophysical applications. Radiative heat transfer can significantly alter the thermal boundary layer and the overall energy distribution in the fluid. The classical differential approximation proposed by Cogley et al. [32] has frequently been used in radiative flow studies, while the fundamental framework for engineering MHD was established by Sutton and Sherman [33]. More recent studies have shown that radiation strongly modifies thermal transport in porous and conducting fluids [1, 3, 8, 11, 14, 19, 20, 23, 24].

Joule heating and viscous dissipation are also important in electrically conducting fluid flows in the presence of magnetic fields. Joule heating arises from the conversion of electrical energy into thermal energy as current flows through the fluid, whereas viscous dissipation represents the conversion of mechanical energy into internal energy due to fluid friction. These effects become especially significant in systems with high electrical conductivity, strong magnetic fields, large velocity gradients, or highly viscous fluids. Their presence usually increases fluid temperature and affects the rate of heat transfer. Several recent investigations have demonstrated the combined influence of Joule heating, viscous dissipation, and radiation in MHD transport problems. For instance, Pradeep and Vijay Kumar [2] analyzed these effects in hybrid nanofluid flow through porous media, while Bhargava et al. [3] studied Joule heating and viscous dissipation in unsteady MHD second-grade fluid flow. Related studies by Basha [9], Lund et al. [13], Sunitha Rani et al. [23], and Preetham and Kumbinarasaiah [16] further confirm that dissipative heating mechanisms are essential for accurately predicting temperature fields in magnetized flows.

In addition to momentum and thermal effects, simultaneous heat and mass transfer in fluids is often governed by cross-diffusion phenomena, namely the Soret and Dufour effects. The Soret effect, or thermal diffusion, is the mass flux generated by temperature gradients, whereas the Dufour effect, or diffusion-thermo effect, is the heat flux induced by concentration gradients. These coupled mechanisms are important in multicomponent fluid mixtures, chemical processing, isotope separation, geophysical flows, and porous-medium transport, where both temperature and concentration gradients are significant. One of the earlier studies highlighting these cross-diffusion effects in unsteady MHD porous-medium flow was conducted by Alam et al. [31]. Since then, many authors have examined Soret and Dufour effects in various MHD configurations, including porous plates, oscillatory flows, and channel problems [1,4,5,10,14,17,20,21,22,25,26,27,34]. These studies indicate that cross-diffusion can substantially alter concentration and temperature distributions and should not be neglected in realistic transport modeling.

Chemical reaction is another important process in heat and mass transfer problems involving reactive species. It has applications in catalytic reactors, fuel cells, corrosion science, polymer engineering, drying processes, combustion systems, and biochemical transport. In the presence of a chemical reaction, concentration profiles are modified not only by convection and diffusion but also by the generation or depletion of species. When a chemical reaction is coupled with magnetic field effects, radiation, and cross-diffusion in a porous medium, the resulting transport process becomes highly nonlinear and physically rich. Recent studies have demonstrated the importance of chemical reaction in radiative and unsteady MHD flows [4, 5, 9, 10, 12, 14, 17, 18, 20, 21, 24, 26, 34]. In particular, Barik et al. [34] considered the effects of chemical reactions on MHD oscillatory flow through a porous medium bounded by vertical porous plates with a heat source and the Soret effect, thereby highlighting the significance of reactive mass transfer in oscillatory porous systems.

Porous media are of considerable practical interest because they occur in packed-bed reactors, groundwater transport, geothermal systems, insulating materials, biological tissues, and filtration devices. The porous structure introduces drag, modifying fluid motion and usually reducing flow velocity, while also influencing heat and mass transport. Several studies have investigated MHD flow and heat transfer in porous channels and related geometries [1,2,6,8,13,20,26,29,31,34]. Jalili et al. [6] examined unsteady MHD fluid flow and heat transfer through porous asymmetric channels, while Aich et al. [8] studied double-diffusive MHD stagnation-point flow in non-Darcy porous media under the effects of radiation. These works highlight the significant roles of permeability and porous resistance in governing overall transport behavior.

A review of the literature shows that many studies have examined individual or partial combinations of the effects of radiation, Joule heating, viscous dissipation, the Soret and Dufour effects, and chemical reaction in MHD flows. However, relatively little attention has been given to MHD oscillatory flow in a channel filled with a porous medium when all these effects are considered simultaneously. Much of the recent literature focuses on boundary-layer flows over vertical plates, stretching sheets, rotating surfaces, wavy channels, and nanofluid models [1–27], whereas fewer studies address the classical oscillatory channel configuration [28–30,34]. Moreover, even within oscillatory flow studies, the simultaneous inclusion of radiative heat transfer, Joule heating, viscous dissipation, Soret-Dufour cross-diffusion, porous resistance, and chemical reaction remains underexplored. This reveals a clear gap in the literature and motivates the present investigation.

The present study therefore examines the effects of radiation, Joule heating, viscous dissipation, and Soret-Dufour effects on MHD oscillatory flow in a channel filled with a porous medium in the presence of a chemical reaction. The combined consideration of these effects is important because they interact strongly: the magnetic field suppresses motion but enhances Joule heating; viscous dissipation increases internal thermal energy; radiation modifies heat transfer; and Soret-Dufour effects couple the thermal and concentration fields, while a chemical reaction alters species transport. The simultaneous influence of these parameters on velocity, temperature, and concentration distributions is of both theoretical and practical significance.

Accordingly, this work aims to develop a comprehensive model of oscillatory MHD channel flow through a porous medium that accounts for the combined effects of radiation, Joule heating, viscous dissipation, Soret diffusion, Dufour diffusion, and chemical reaction. The study is expected to provide useful insights into how the governing dimensionless parameters influence transport behavior and to contribute to a broader understanding of coupled heat and mass transfer in electrically conducting fluids flowing through porous structures. Such results may inform the design of thermal systems, MHD devices, chemical processing equipment, and porous-transport applications involving oscillatory forcing and reactive-species transport.

2. Mathematical Analysis

An unsteady two-dimensional convective heat and mass transfer flow of a viscous, incompressible, electrically conducting, and optically thin fluid in a channel filled with saturated porous medium with chemical reaction is considered. A uniform, applied, homogeneous magnetic field is imposed in the transverse direction. It is assumed that the fluid has low electrical conductivity and that the induced magnetic field is negligible compared with the applied magnetic field. The fluid is also assumed to undergo a homogeneous first-order chemical reaction. In addition, the effects of thermal radiation, heat source/sink, viscous dissipation, Joule heating, the Soret and Dufour effects are taken into account. A Cartesian coordinate system (x', y') is chosen such that the x'-axis lies along the centreline of the channel and the y'-axis is normal to it. Under the usual Boussinesq approximation, the governing equations of the flow are as follows.

Momentum equation

$$\frac{\partial u'}{\partial t'} = -\frac{1}{\rho}\frac{\partial P'}{\partial x'} + \nu\frac{\partial^2 u'}{\partial y'^2} - \frac{\nu}{K'}u' - \frac{\sigma_e B_0^2}{\rho}u' + g\beta(T' - T_0') + g\beta^*(C' - C_0') \quad (1)$$

Energy equation

$$\frac{\partial T'}{\partial t'} = \frac{\kappa}{\rho c_p}\left(\frac{\partial^2 T'}{\partial y'^2}\right) - \frac{1}{\rho c_p}\left(\frac{\partial q_r}{\partial y'}\right) + \frac{Q_0}{\rho c_p}(T' - T_0') + \frac{\mu}{\rho c_p}\left(\frac{\partial u'}{\partial y'}\right)^2 + \frac{\sigma_e B_0^2}{\rho c_p}u'^2 + \frac{D_m K_T}{C_s \rho c_p}\left(\frac{\partial^2 C'}{\partial y'^2}\right) \quad (2)$$

Species equation

$$\frac{\partial C'}{\partial t'} = D\left(\frac{\partial^2 C'}{\partial y'^2}\right) - K_r'(C' - C_0') + \frac{D_m K_T}{T_m}\left(\frac{\partial^2 T'}{\partial y'^2}\right) \quad (3)$$

The boundary conditions for the velocity, temperature and concentration fields remain unchanged and are given by

$$u' = 0,\ T' = T_w',\ C' = C_w' \quad on\ y' = 1 \quad (4)$$
$$u' = 0,\ T' = T_0',\ C' = C_0' \quad on\ y' = 0$$

where u' is the axial velocity, t' - the time, T' - the fluid temperature, P' - the pressure, g- the gravitational force, q_r - the radiative heat flux , β and β^* - the coefficient of volume expansion due to temperature and concentration , c_p - the specific heat at constant pressure, κ the thermal conductivity, K' - the porous medium permeability coefficient, $Bo = (\mu_e H_0)$ - the electromagnetic induction, μ_e - the magnetic permeability, *Ho* - the intensity of magnetic field, σ_e - the conductivity of the fluid, ρ - the fluid density and ν - the kinematic viscosity coefficient.

It is assumed that the temperatures of the walls T_0' and $T^{w\prime}$ are sufficiently high to induce radiative heat transfer. Following the optically thin approximation of Cogley et al., the radiative heat flux is taken as

$$\frac{\partial q_r}{\partial y'} = 4\alpha^2\left(T_0' - T'\right) \quad (5)$$

where α is the mean radiation absorption coefficient.

To convert the governing equations into non-dimensional form, the following variables are introduced:

$$x = \frac{x'}{a}, y = \frac{y'}{a}, u = \frac{u'}{U}, t = \frac{t'U}{a}, \theta = \frac{T' - T_0'}{T_w' - T_0'}, \phi = \frac{C' - C_0'}{C_w' - C_0'}, P = \frac{aP'}{\rho\nu U} \quad (7)$$

The non-dimensional parameters are

$$Re = \frac{Ua}{\nu}, Da = \frac{K'}{a^2}, H^2 = \frac{\sigma_e B_0^2 a^2}{\rho\nu}, Gr = \frac{g\beta(T_w' - T_0')a^2}{\nu U}, Gc = \frac{g\beta^*(C_w' - C_0')a^2}{\nu U}$$
$$Pe = \frac{Ua\rho c_p}{k}, Sc = \frac{\nu}{D}, K_r = \frac{K_r' a}{U}, N^2 = \frac{4\alpha^2 a^2}{k}, Q = \frac{Q_0 a^2}{k}, Br = \frac{\mu U^2}{k(T_w' - T_0')} \quad (8)$$
$$Du = \frac{D_m K_T(C_w' - C_0')}{C_s k(T_w' - T_0')}, Sr = \frac{D_m K_T(T_w' - T_0')}{DT_m(C_w' - C_0')}$$

Where, ***U*** is the flow mean velocity and ***a*** being the width of the channel.

In view of the Eq. (6), the equations (1) – (3) reduce to the following dimensionless form.

Dimensionless momentum equation

$$\text{Re}\frac{\partial u}{\partial t} = -\frac{\partial P}{\partial x} + \frac{\partial^2 u}{\partial y^2} - (s^2 + H^2)u + +Gr\theta + Gc\phi \quad (9)$$

Dimensionless energy equation

$$Pe\frac{\partial\theta}{\partial t} = \frac{\partial^2\theta}{\partial y^2} + N^2\theta + Q\theta + Br\left(\frac{\partial u}{\partial y}\right)^2 + BrH^2u^2 + Du\left(\frac{\partial^2\phi}{\partial y^2}\right) \quad (10)$$

Dimensionless species equation

$$\frac{\partial\phi}{\partial t} = \left(\frac{1}{ScRe}\right)\left(\frac{\partial^2\phi}{\partial y^2}\right) + \left(\frac{Sr}{ScRe}\right)\frac{\partial^2\theta}{\partial y^2} - Kr\phi \quad (11)$$

The corresponding dimensionless boundary conditions are

$$u = 0, \theta = 1, \phi = 1 \quad on\ y = 1 \quad (12)$$
$$u = 0, \theta = 0, \phi = 0 \quad on\ y = 0$$

Here, Gr and Gc are the thermal and solutal Grashof numbers, H is the Hartmann number, Da is the Darcy number, Pe is the Peclet number, Re is the Reynolds number, Sc is the Schmidt number, Kr is the chemical reaction parameter, N is the radiation parameter, Q is the heat source/sink parameter, Br is the Brinkman number representing viscous dissipation, Du is the Dufour number, and Sr is the Soret number.

3. Solution of the Problem

In order to solve equations (9) - (12) numerically in Mathematica using NDSolveValue with the Method of Lines under an oscillatory pressure-gradient forcing for purely oscillatory flow, let

Graph-wise Results and Discussion

Fig. 1. Effect of Re on velocity

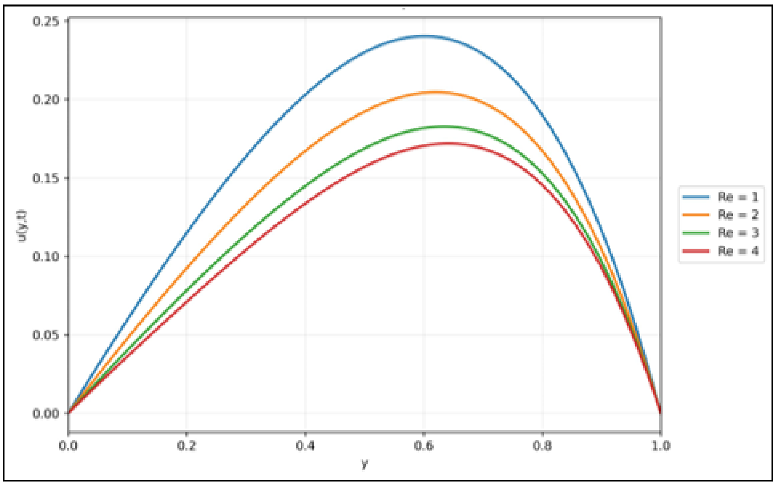

Figure 1: Effect of Re on velocity at t = 10

The velocity profile decreases consistently as Re increases from 1 to 4. The reduction is most evident in the channel's central region, where the peak velocity decreases while the basic profile shape remains unchanged. This indicates that, within the present model, a larger Reynolds number weakens the fluid motion rather than enhancing it. The curves still satisfy the same boundary behavior at y = 0 and y = 1, so the main effect of Re is on the magnitude of the flow field.

Fig. 2. Effect of Da on velocity

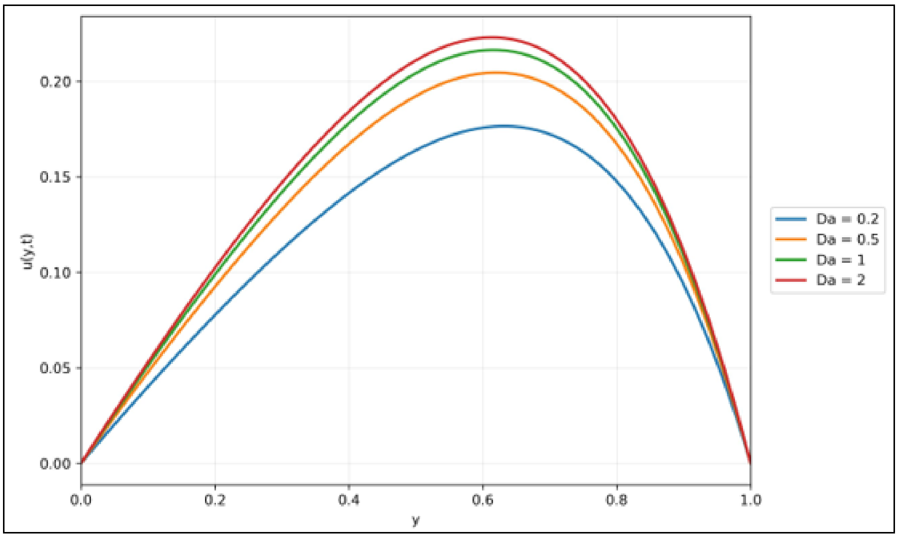

Figure 2: Effect of Da on velocity at t = 10

An increase in Da from 0.2 to 1.0 increases the velocity profile throughout the domain, indicating that permeability-related effects support fluid motion. However, when Da is increased further to 2.0, the curve drops slightly below the Da = 1.0 case, although it remains above the low-Da profiles. This suggests a non-linear response with the strongest enhancement occurring around the intermediate value used here. The peak remains near the channel interior, and the profile remains smooth.

Fig. 3. Effect of Ha on velocity

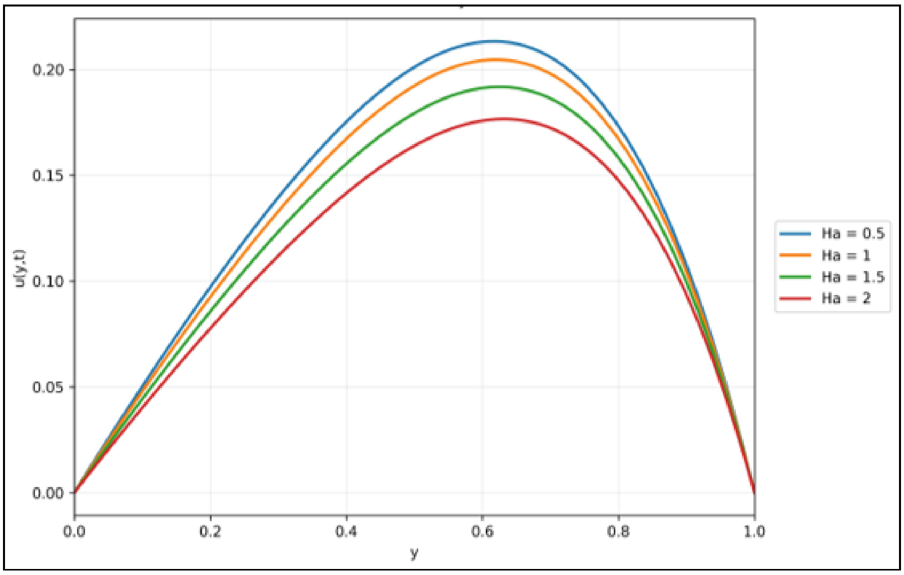

Figure 3: Effect of Ha on velocity at t = 10

The velocity decreases as Ha increases from 0.5 to 2.0. This is evident from the downward shift of the entire profile and the reduction in the maximum velocity in the core region. The result is consistent with the magnetic field's damping role, since a higher Hartmann number generally strengthens the Lorentz force and resists the flow. Thus, increasing Ha suppresses momentum transport in the present configuration.

Fig. 4. Effect of Gr on velocity

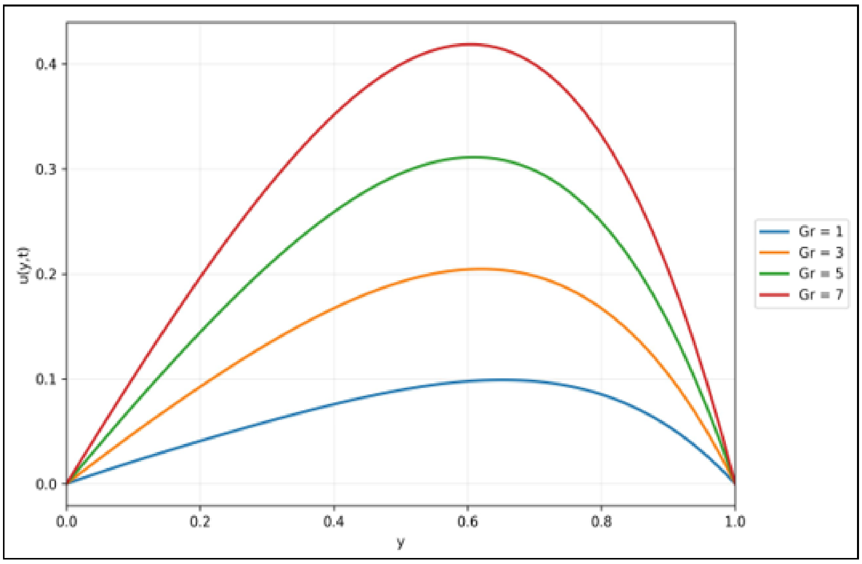

Figure 4: Effect of Gr on velocity at t = 10

The velocity rises strongly with increasing Gr, and the separation between the curves is large over most of the domain. Higher Gr yields a much larger peak velocity, indicating that thermal buoyancy significantly accelerates the flow. The boundary values remain unchanged, while the interior response strengthens. Therefore, Gr is a major parameter enhancing the velocity field in this study.

Fig. 5. Effect of Gc on velocity

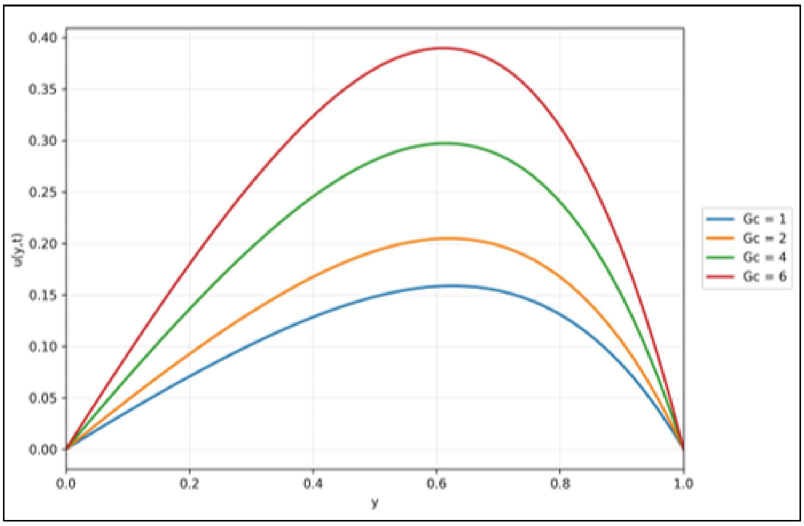

Figure 5: Effect of Gc on velocity at t = 10

The velocity profile increases monotonically as Gc increases from 1 to 6. The improvement is pronounced in the mid-region, where the peak velocity for Gc = 6 is substantially larger than that for Gc = 1. This behavior indicates that concentration-induced buoyancy enhances fluid motion. Hence, larger Gc strengthens the solutal driving force and elevates the velocity distribution.

Fig. 6. Effect of Pe on temperature

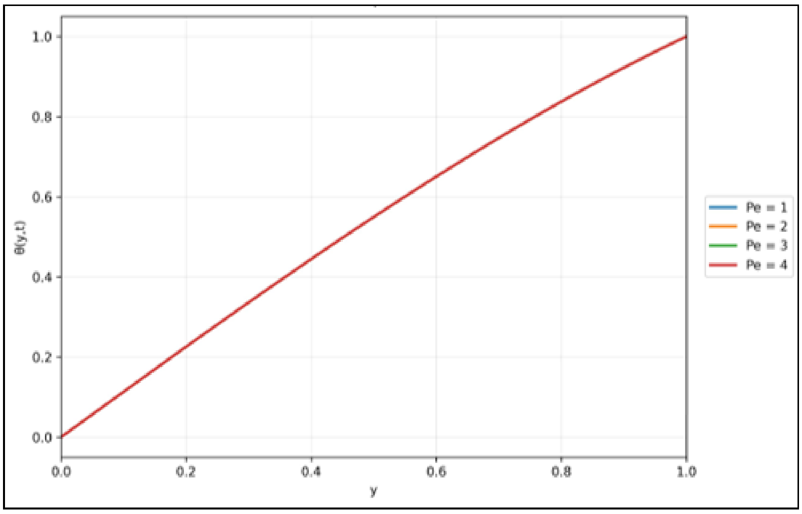

Figure 6: Effect of Pe on temperature at t = 10

All temperature curves overlap, forming a nearly linear profile from y = 0 to y = 1. Within the plotted parameter range, changing Pe from 1 to 4 does not produce any visible change in the temperature field. This means the influence of Pe is negligible under the selected conditions, or at least too small to be observed on the present scale. The temperature distribution, therefore, remains almost unchanged across the range of Pe values tested.

Fig. 7. Effect of Sc on concentration

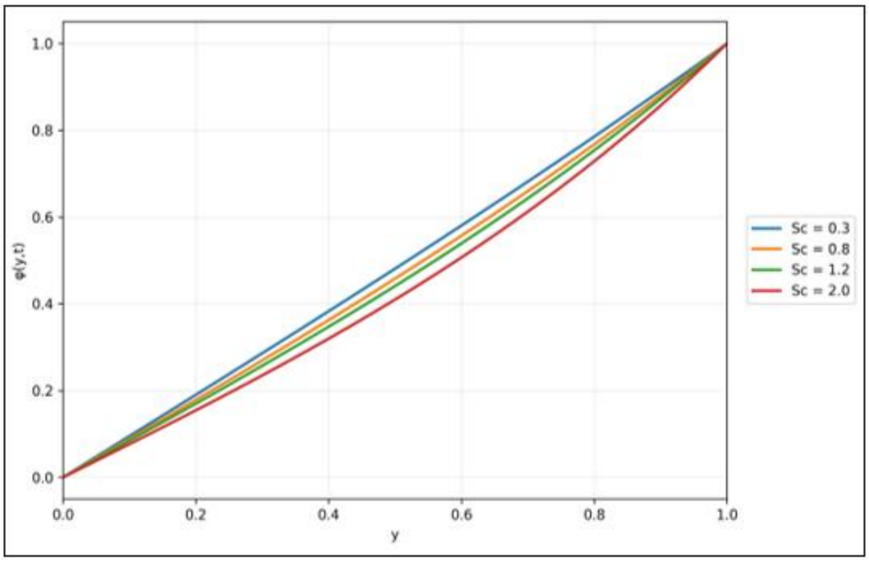

Figure 7: Effect of Sc on concentration at t = 10

The concentration profile decreases gradually as Sc increases from 0.3 to 2.0. The effect is small near the boundaries but becomes more pronounced in the interior, where higher Sc yields lower concentration values. This indicates a thinning of the concentration field as mass diffusivity-related effects become weaker relative to momentum diffusion. Consequently, a larger Schmidt number suppresses the concentration distribution in the present problem.

Fig. 8. Effect of Kr on concentration

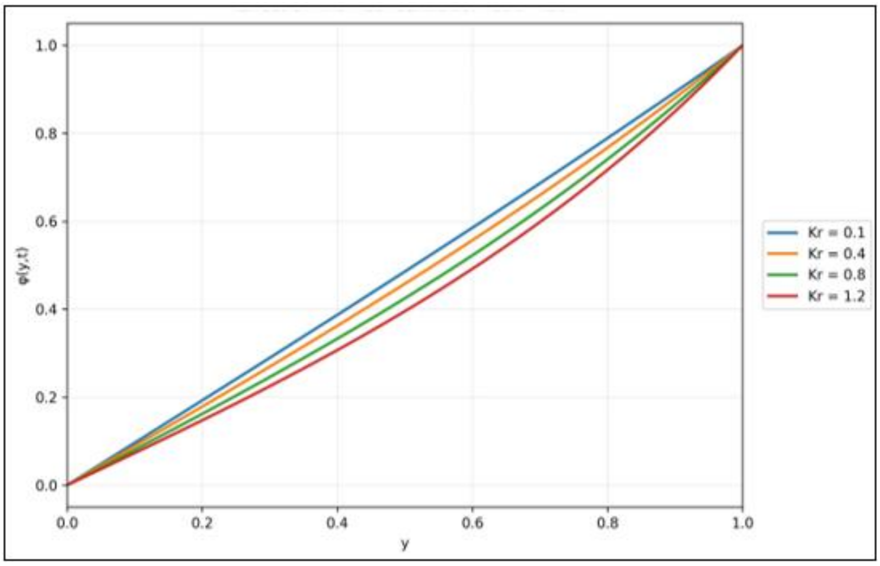

Figure 8: Effect of Kr on concentration at t = 10

Result and discussion: Increasing Kr lowers the concentration profile across the domain, with the biggest differences appearing away from the boundaries. The Kr = 1.2 curve lies below the other cases, while Kr = 0.1 gives the highest concentration. This trend is typical of a destructive chemical reaction parameter, since a stronger reaction consumes the species more rapidly. Thus, a larger Kr reduces species concentration and shrinks the concentration boundary layer.

Fig. 9. Effect of Nr on temperature

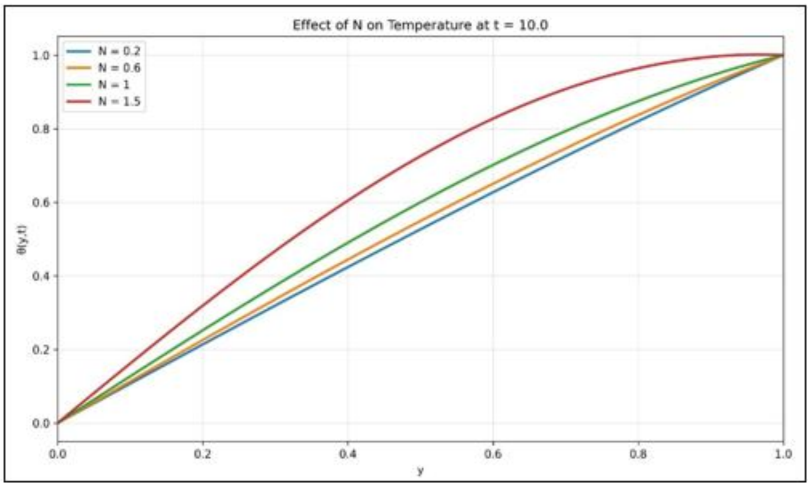

Figure 9: Effect of N on temperature at t = 10

Result and discussion: The temperature profile increases noticeably with increasing N. The rise is especially pronounced in the mid-region, where higher N pushes the curve upward, producing a thicker thermal layer. Among the tested values, N = 1.5 yields the strongest thermal response. Therefore, thermal radiation represented by N enhances the temperature field in this model.

Fig. 10. Effect of Q on temperature

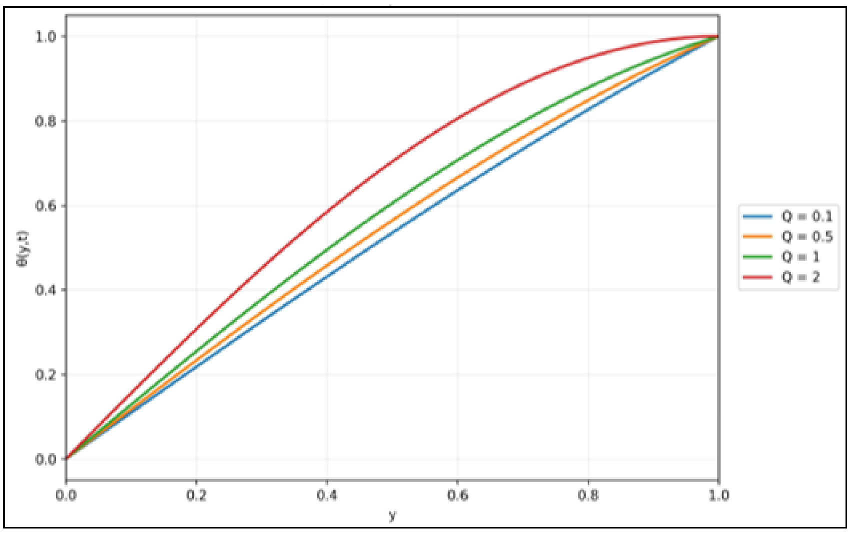

Figure 10: Effect of Q on temperature at t = 10

Result and discussion: The temperature increases as Q rises from 0.1 to 2.0, and the enhancement becomes more pronounced in the upper half of the domain. Higher Q lifts the entire profile and causes the solution to approach the upper boundary value more rapidly. This behavior indicates that internal heat generation supplies extra thermal energy to the system. Hence, Q acts as a heating parameter that intensifies the temperature distribution.

Fig. 11. Effect of Br on temperature

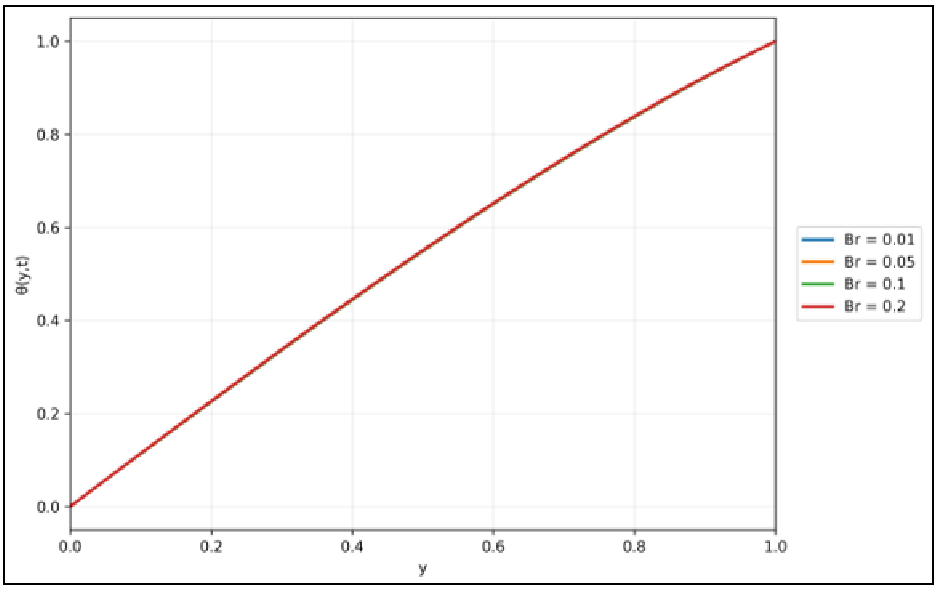

Figure 11: Effect of Br on temperature at t = 10

Result and discussion: The curves for all values of Br are almost exactly superimposed, producing the same linear temperature profile. This indicates that the Brinkman number has no discernible effect on the temperature distribution over the selected parameter range. Any viscous dissipation effect present in the formulation is therefore extremely small under these conditions. In practical terms, the temperature field may be treated as insensitive to Br in the current graph set.

Fig. 12. Effect of Du on temperature

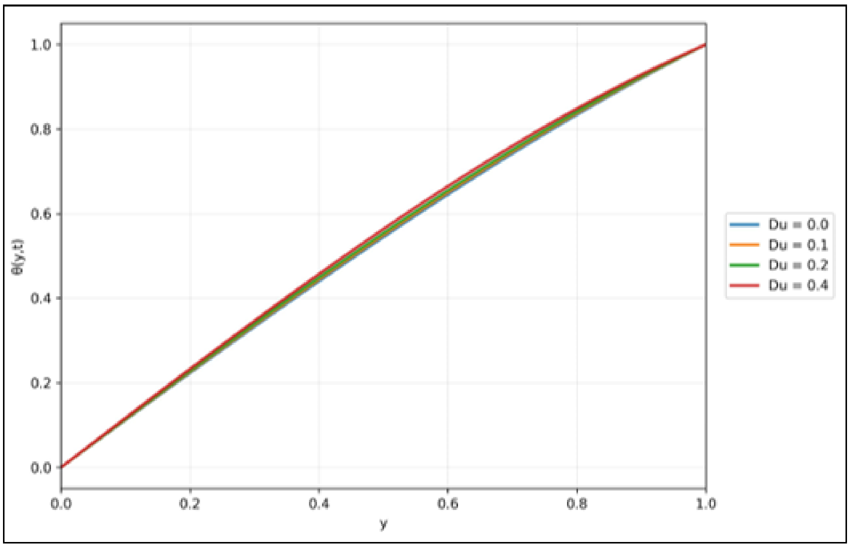

Figure 12: Effect of Du on temperature at t = 10

Result and Discussion: The temperature profiles for different Du values are very similar, but a slight increase is still evident as Du increases from 0.0 to 0.4. The response is subtle and primarily evident in the slight upward separation of the higher-Du curves. This implies that the Dufour effect enhances heat transfer, though its influence is weaker than that of parameters such as Nr or Q. Thus, Du causes only a mild temperature enhancement in the present range.

Fig. 13. Effect of Sr on concentration

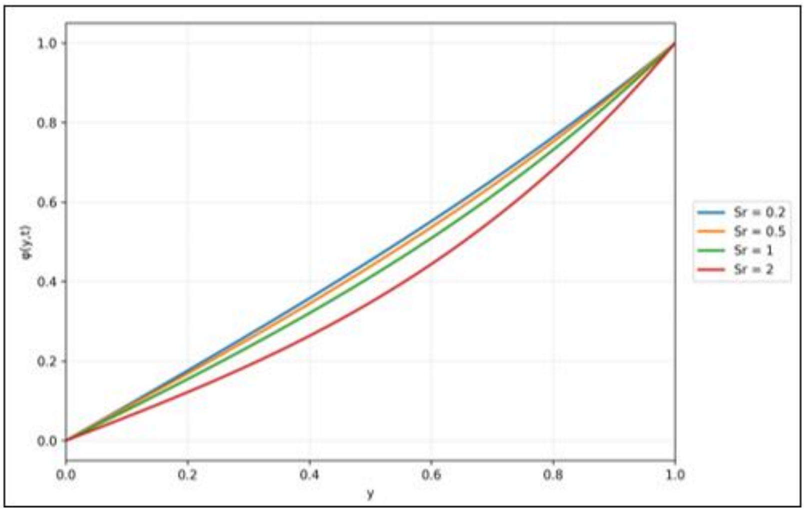

Figure 13: Effect of Sr on concentration at t = 10

Result and Discussion: The concentration profile decreases as Sr increases from 0.2 to 2.0. The reduction is modest near the boundaries and clearer in the interior, where the higher-Sr curves lie lower. Based on the plot, the Soret parameter suppresses the magnitude of the concentration under the chosen conditions. Therefore, increasing Sr weakens the concentration field and slightly reduces the concentration boundary-layer thickness.

Fig. 14. Effect of A_0 on velocity

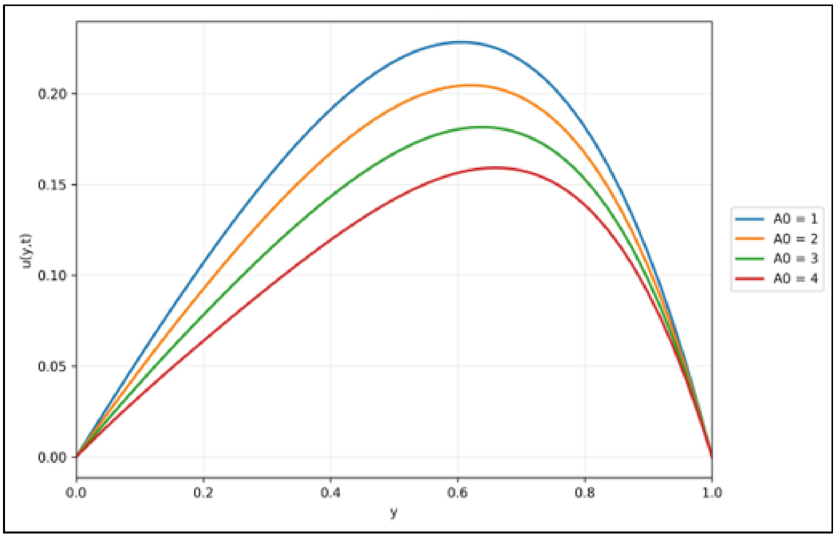

Figure 14: Effect of A_0 on velocity at t = 10

Result and discussion: The velocity profile decreases steadily as increases from 1 to 4. Each successive increase in shifts the curve downward and lowers the peak velocity, while the overall parabolic-like shape is preserved. This indicates that has a retarding effect on the fluid motion in the current formulation. The effect is strongest around the central region, where the gap between the curves is most visible.

Fig. 15. Effect of ω on velocity

Paper ID: SR26723172037 DOI: https://dx.doi.org/10.21275/SR26723172037

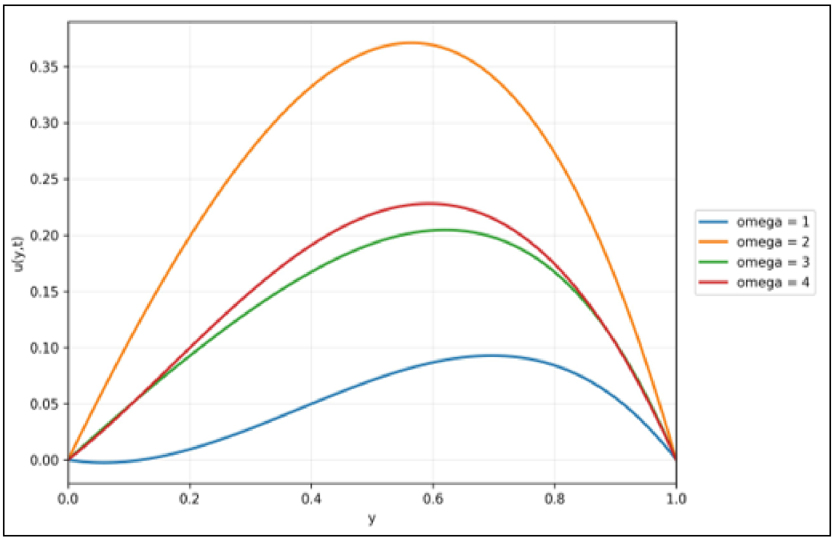

Figure 15: Effect of ω on velocity at t = 10

Result and discussion: The influence of ω is non-monotonic. The velocity rises sharply from ω = 1 to ω = 2 and reaches its highest peak at ω = 2, after which it decreases for ω = 3 and ω = 4. Even so, the ω = 3 and ω = 4 cases remain above the ω = 1 profile over much of the domain. This suggests the presence of an optimal oscillatory effect within the tested range, where a moderate ω yields the strongest flow response.

4. Overall Physical Interpretation

Taken together, the present model shows that the channel transport is controlled by a competition between resistive effects $(Ha, Da^{-1}, Kr)$and source/buoyancy effects $(Gr, Gc, Nr, Q, Br, Du, Sr)$. The strongest thermal loading occurs when radiation, internal heating, viscous dissipation, and Ohmic heating act simultaneously. The strongest species attenuation occurs when chemical reaction dominates the Soret-driven replenishment of concentration. From an applications standpoint, the model is especially relevant where oscillatory transport coexists with electromagnetic control, porous resistance, and coupled heat/mass diffusion, such as compact heat exchangers, porous reactors, thermal processing systems, and certain biomedical transport problems.

Table 1: Skin-friction coefficients for the baseline case

t	C_f at y= 0	C_f at y= 1
0	0.000000	0.000000
1	-0.028705	-0.7654
2	1.22718	-2.02139
3	0.0961432	-0.890263
4	1.08307	-1.87726
5	0.260031	-1.05417
6	0.902753	-1.69692
7	0.453332	-1.24749
8	0.700585	-1.49474
9	0.660599	-1.45478
10	0.492688	-1.28682

Skin-friction coefficients for different values of Re at t = 10

Re	C_f at y= 0	C_f at y= 1
1	0.614913	-1.41045
2	0.492688	-1.28682
3	0.415066	-1.20782
4	0.357595	-1.14767

Skin-friction coefficients for different values of Ha at t = 10

Ha	C_f at y= 0	C_f at y= 1
0.5	0.517135	-1.32053
1.0	0.492688	-1.28682
1.5	0.45702	-1.23637
2.0	0.415281	-1.1752

Skin-friction coefficients for different values of Da at t = 10

Da	C_f at y= 0	C_f at y= 1
0.2	0.415197	-1.1751
0.5	0.492688	-1.28682
1.0	0.525977	-1.33254
2.0	0.544626	-1.35762

Skin-friction coefficients for different values of Gr at t = 10

Gr	C_f at y= 0	C_f at y= 1
1.0	0.224362	-0.697805
3.0	0.492688	-1.28682
5.0	0.762172	-1.87713
7.0	1.03377	-2.46976

Skin-friction coefficients for different values of Gc at t = 10

Gc	C_f at y= 0	C_f at y= 1
1.0	0.379973	-1.01751
2.0	0.492688	-1.28682
4.0	0.718273	-1.8256
6.0	0.944052	-2.36459

Skin-friction coefficients for different values of Kr at t = 10

Kr	C_f at $y=0$	C_f at $y=1$
0.1	0.503638	-1.29986
0.4	0.492688	-1.28682
0.8	0.479622	-1.27104
1.2	0.468067	-1.25685

Skin-friction coefficients for different values of Nr at t = 10

Nr	C_f at $y=0$	C_f at $y=1$
0.2	0.477585	-1.2693
0.6	0.492688	-1.28682
1.0	0.526453	-1.32553
1.5	0.610549	-1.41974

Skin-friction coefficients for different values of Q at t = 10

Q	C_f at $y=0$	C_f at $y=1$
0.1	0.483117	-1.27574
0.5	0.502691	-1.29835
1.0	0.529897	-1.32944
2.0	0.595861	-1.40347

Skin-friction coefficients for different values of B_r at t = 10

B_r	C_f at $y=0$	C_f at $y=1$
0.01	0.49235	-1.28642
0.05	0.492688	-1.28682
0.1	0.493095	-1.2873
0.2	0.493901	-1.28825

Skin-friction coefficients for different values of Du at t = 10

Du	C_f at $y=0$	C_f at $y=1$
0.0	0.489665	-1.28328
0.1	0.492688	-1.28682
0.2	0.495746	-1.29041
0.4	0.502088	-1.29785

Skin-friction coefficients for different values of Sr at t = 10

S_r	C_f at $y=0$	C_f at $y=1$
0.2	0.490804	-1.2846
0.5	0.484926	-1.27769
1.0	0.474258	-1.26514
2.0	0.448851	-1.23526

Skin-friction coefficients for different values of A_0 at t = 10

A_0	C_f at $y=0$	C_f at $y=1$
1.0	0.560321	-1.35447
2.0	0.492688	-1.28682
3.0	0.425196	-1.21931
4.0	0.357898	-1.152

Skin-friction Coefficients for different values of ω at t = 10

ω	C_f at $y=0$	C_f at $y=1$
1.0	-0.0898229	-0.704265
2.0	1.10174	-1.89596
3.0	0.492688	-1.28682
4.0	0.421676	-1.21583

References

[1] Goud BS, Aparna M, Nisar KS. *Influence of Dufour, Soret and radiation on unsteady MHD flow through a porous media past an infinite inclined vertical plate with ohmic heating: Numerical study.* Results in Engineering. 2025. doi:10.1016/j.rineng.2025.106673

[2] Pradeep S, Vijay Kumar P. *Impact of Joule heating, viscous dissipation and radiation on magnetohydrodynamic hybrid nanofluid flow over a vertical plate in the porous medium: An analytical approach.* Results in Engineering. 2025;28:107911. doi:10.1016/j.rineng.2025.107911

[3] Ch Bhargava KNV, Ibrahim SM, Kodi R. *Effects of hall current, radiation absorption and diffusion thermo on an unsteady MHD flow of second grade fluid through porous media in the presence of joule heating and viscous dissipation.* Multiscale and Multidisciplinary Modeling, Experiments and Design. 2025;8:260. doi:10.1007/s41939-025-00842-y

[4] Prashanth M, Srinivasa Rao V. *The impact of soret, Dufour, and chemical reaction on MHD nanofluid over a stretching sheet.* Partial Differential Equations in Applied Mathematics. 2024. doi:10.1016/j.padiff.2024.100674

[5] Reddy MS, Kumar MA. *Influence of magnetic field chemical reaction and Soret-Dufour parameters on Maxwell nanofluid flow over a porous vertical stretching surface: A numerical study.* Case Studies in Chemical and Environmental Engineering. 2024. doi:10.1016/j.cscee.2024.100958

[6] Jalili B, Azar AA, Jalili P, Liu D, Abdelmohimen MAH, Domiri Ganji D. *Investigation of the unsteady MHD fluid flow and heat transfer through the porous medium asymmetric wavy channel.* Case Studies in Thermal Engineering. 2024;61:104859. doi:10.1016/j.csite.2024.104859

[7] Disu AB, Oyelami OA, Oyelakin IS, Salawu SO. *Heat transfer on MHD oscillatory flow in a vertical double-passage channel.* Science World Journal. 2024;19(3):766–771. doi:10.4314/swj.v19i3.23

[8] Aich W, Abbas A, Obalalu AM, Hassen W, Said LB, Hajlaoui R, Kolsi L. *Double diffusive MHD stagnation point flow of second-grade fluid in non-Darcy porous media under radiation effects.* Scientific Reports. 2025;15:395. doi:10.1038/s41598-024-84562-2

[9] Basha H. *Dynamics of chemically reactive magnetized Casson nanofluid flow over a sensor surface under joule heating and viscous dissipation effects.* BioNanoScience. 2024; 14: 241–267. doi:10.1007/s12668-023-01231-w

[10] Bormudoi M, Ahmed N. *Convective MHD flow of a rotating fluid past through a moving isothermal plate under diffusion-thermo and radiation absorption.* Journal of Heat and Mass Transfer Research. 2023;10(2):245–256. doi:10.22075/JHMTR.2023.31013.1454

[11] Deepthi VVL, Lashin MAM, Ravi Kumar N, Raghunath K, Ali F, Oreijah M, Guedri K, Tag-ElDin ESM, Ijaz Khan M, Galal Ahmed M. *Recent development of heat and mass transport in the presence of hall, ion slip and thermo diffusion in radiative second grade material: application of micromachines.*

Micromachines. 2022; 13: 1566. doi:10.3390/mi13101566

[12] Hari Babu K, Raghunath K, Charankumar G, Lorenzini G. *Heat and mass transfer on unsteady MHD chemically reacting rotating flow of Jeffrey fluid past an inclined plate under the impact of hall current, diffusion thermo, and radiation absorption.* Journal of Advanced Research in Fluid Mechanics and Thermal Sciences. 2023;111(2):225–241. doi:10.7934/arfmts.111.2.225241

[13] Lund LA, Yashkun U, Shah NA. *Multiple solutions of unsteady Darcy-Forchheimer porous medium flow of Cu–Al2O3/water-based hybrid nanofluid with Joule heating and viscous dissipation effect.* Journal of Thermal Analysis and Calorimetry. 2024; 149: 2303–2315. doi:10.1007/s10973-023-12819-5

[14] Omar TB, Raghunath K, Ali F, Khalid M, Tag-ElDin ESM, Oreijah M, Guedri K, Khedher NB, Ijaz Khan M. *Hall current and soret effects on unsteady MHD rotating flow of second-grade fluid through porous media under the influences of thermal radiation and chemical reactions.* Catalysts. 2022;12:1233. doi:10.3390/catal12101233

[15] Prasad VR, Varma NUB, Jamuna B, Suresh MS, Sudhakaru K, Raghunath K. *Effects of Hall current and thermal diffusion on unsteady MHD rotating flow of water-based Cu and TiO2 nanofluid in the presence of thermal radiation and chemical reaction.* Multiscale and Multidisciplinary Modeling, Experiments and Design. 2025;8:161. doi:10.1007/s41939-025-00736-z

[16] Preetham MP, Kumbinarasaiah S. *Significance of Arrhenius activation energy on three-dimensional unsteady nanofluid flow with nonlinear thermal radiation and Joule heating via wavelet technique.* Journal of Mathematical Chemistry. 2025; 63: 456–473. doi:10.1007/s10910-024-01680-y

[17] Raghunath K, Mohanaramana R. *Hall, Soret, and rotational effects on unsteady MHD rotating flow of a second-grade fluid through a porous medium in the presence of chemical reaction and aligned magnetic field.* International Communications in Heat and Mass Transfer. 2022; 137: 106287. doi:10.1016/j.icheatmasstransfer.2022.106287

[18] Raghunath K, Mohanaramana R, Nagesh G, Charankumar G, Khan SU, Ijaz Khan M. *Hall and ion slip radiative flow of chemically reactive second-grade fluid through porous saturated space via perturbation approach.* Waves in Random and Complex Media. 2022. doi:10.1080/17455030.2022.2108555

[19] Raghunath K, Mohana Ramana R, Veeranna V, Ijaz Khan M, Abdullaev S, Tamam N. *Hall current and thermal radiation effects of 3D rotating hybrid nanofluid reactive flow via stretched plate with internal heat absorption.* Results in Physics. 2023; 53: 106915. doi:10.1016/j.rinp.2023.106915

[20] Raghunath K, Ramachandra Reddy V, Ijaz Khan M, Abdullaev SS, Habibullah AB, Boujelbene M, Bouazzi Y. *Unsteady magneto-hydrodynamics flow of Jeffrey fluid through porous media with thermal radiation, Hall current, and Soret effects.* Journal of Magnetism and Magnetic Materials. 2023;582:171033. doi:10.1016/j.jmmm.2023.171033

[21] Raghunath K, Mohana Ramana R, Ramachandra Reddy V, Obulesu M. *Diffusion thermo and chemical reaction effects on magnetohydrodynamic Jeffrey nanofluid over an inclined vertical plate in the presence of radiation absorption and constant heat source.* Journal of Nanofluids. 2023;12:147–156. doi:10.1166/jon.2023.1923

[22] Ramachandra Reddy V, Sreedhar G, Raghunath K. *Effects of hall current, activation energy, and diffusion thermo of MHD Darcy-Forchheimer Casson nanofluid flow in the presence of Brownian motion and thermophoresis.* Journal of Advanced Research in Fluid Mechanics and Thermal Sciences. 2023;105(2):129–145. doi:10.37934/arfmts.105.2.129145

[23] Sunitha Rani Y, Kalyan Kumar P, Raghunath K, Asmat F. *Unsteady MHD rotating mixed convective flow through an infinite vertical plate subject to Joule heating, thermal radiation, Hall current, radiation absorption.* Journal of Thermal Analysis and Calorimetry. 2024;149:8813–8826. doi:10.1007/s10973-024-12954-7

[24] Suresh Kumar Y, Hussain S, Raghunath K, Ali F, Guedri K, Eldin SM, Ijaz Khan M. *Numerical analysis of magnetohydrodynamics Casson nanofluid flow with activation energy, Hall current, and thermal radiation.* Scientific Reports. 2023;13:4021. doi:10.1038/s41598-023-28379-5

[25] Kavitha R, Ladu NSD, Ravi S. *Soret Effect and Chemical Process on MHD Oscillatory Flow in a Physiological Fluid.* Applied Bionics and Biomechanics. 2025;2025:8818822. doi:10.1155/abb/8818822

[26] Kumar VV, Raja Shekar MN, Bejawada SG. *Role of Soret, Dufour Influence on Unsteady MHD Oscillatory Casson Fluid Flow an Inclined Vertical Porous Plate in the Existence of Chemical Reaction.* Journal of Advanced Research in Fluid Mechanics and Thermal Sciences. 2023;110(2):157–175. doi:10.37934/arfmts.110.2.157175

[27] Noor NAM, Shafie S, Hamed YS, Admon MAS. *Soret and Dufour Effects on MHD Squeezing Flow of Jeffrey Fluid in Horizontal Channel with Thermal Radiation.* PLOS ONE. 2022. doi:10.1371/journal.pone.0266494

[28] Misra JC, Adhikary SD. *MHD Oscillatory Channel Flow, Heat and Mass Transfer in a Physiological Fluid in the Presence of Chemical Reaction.* Alexandria Engineering Journal. 2016;55(1):287–297. doi:10.1016/j.aej.2015.10.005

[29] Makinde OD, Mhone PY. *Heat transfer to MHD oscillatory flow in a channel filled with porous medium.* Romanian Journal of Physics. 2005;50(9–10):931–938

[30] Muthuraj R, Srinivas S. *A note on heat transfer to MHD oscillatory flow in an asymmetric wavy channel.* International Communications in Heat and Mass Transfer. 2010;37:1255–1260

[31] Alam MS, Rahman MM, Samad MA. *Dufour and Soret Effects on Unsteady MHD Free Convection and Mass Transfer Flow past a Vertical Porous Plate in a Porous Medium.* Nonlinear Analysis: Modelling and Control. 2006;11(3):217–226. doi:10.15388/NA.2006.11.3.14743

[32] Cogley ACL, Vincenti WG, Giles ES. *Differential approximation to radiative heat transfer in a nongrey gas near equilibrium.* AIAA Journal. 1968;6:551–553

[33] Sutton GW, Sherman A. *Engineering Magnetohydrodynamics.* New York: McGraw-Hill; 1965

[34] Barik RN, Dash GC, Mohanty A. *Chemical reaction effect on MHD oscillatory flow through a porous medium bounded by two vertical porous plates with heat source and Soret effect.* Journal of Applied Analysis and Computation. 2013.